Methane emissions from Amazonian Rivers and their contribution to the global methane budget

Henrique O. Sawakuchi, David Bastviken, Andre O. Sawakuchi, Alex V. Krusche, Maria V. R. Ballester and Jeffrey E. Richey

Original Publication:

Henrique O. Sawakuchi, David Bastviken, Andre O. Sawakuchi, Alex V. Krusche, Maria V. R. Ballester and Jeffrey E. Richey, Methane emissions from Amazonian Rivers and their contribution to the global methane budget, 2014, Global Change Biology, (20), 9, 2829-2840.
http://dx.doi.org/10.1111/gcb.12646

Title: **Methane emissions from Amazonian Rivers and their contribution to the global methane budget**

Running head: **Methane emissions from Amazonian Rivers**

Henrique O. Sawakuchi[1*], David Bastviken[2], André O. Sawakuchi[3], Alex V. Krusche[1], Maria Victoria R. Ballester[1], Jeffrey E. Richey[4]

[1]Environmental Analysis and Geoprocessing Laboratory, Center for Nuclear Energy in Agriculture, University of São Paulo, Av. Centenário, 303, Piracicaba, SP 13400-970, Brazil;[2]Department of Thematic Studies – Water and Environmental Studies, Linköping University, Linköping, SE-581 83, Sweden;[3]Departament of Sedimentary and Environmental Geology, Institute of Geosciences, University of São Paulo, Rua do Lago, 562, São Paulo, SP 05508-080, Brazil;[4]School of Oceanography, University of Washington, Seattle, WA 98195-7940, USA.

*Corresponding author: Henrique O. Sawakuchi

Phone: +55 19 34294076; Fax: +55 19 34294059

e-mail: henrique.sawakuchi@usp.br

Keywords: methane flux, CH_4, ebullition, tropical rivers, Amazon, greenhouse gas, natural emission.

Type of paper: Primary Research Articles

Abstract

Methane (CH_4) fluxes from world rivers are still poorly constrained, with measurements restricted mainly to temperate climates. Additional river flux measurements, including spatio-temporal studies, are important to refine extrapolations. Here we assess the spatio-temporal variability of CH_4 fluxes from the Amazon and its main tributaries, the Negro, Solimões, Madeira, Tapajós, Xingu, and Pará Rivers, based on direct measurements using floating chambers. Sixteen out of 34 sites were measured during low and high water seasons. Significant differences were observed within sites in the same river and among different rivers, types of rivers, and seasons. Ebullition contributed to more than 50% of total emissions for some rivers. Considering only river channels, our data indicate that large rivers in the Amazon Basin release between 0.40 and 0.58 Tg CH_4 yr^{-1}. Thus, our estimates of CH_4 flux from all tropical rivers and rivers globally were, respectively, 19-51% to 31-84% higher than previous estimates, with large rivers of the Amazon accounting for 22-28% of global river CH_4 emissions.

Introduction

Despite their small areal extent inland waters play an important role in regional and global carbon balances as sources of both CO_2 (Battin *et al.*, 2009, Cole *et al.*, 2007, Richey *et al.*, 2002, Tranvik *et al.*, 2009) and CH_4 (Bastviken *et al.*, 2011). Recent estimates show that inland waters outgas around 2.1 Pg C yr^{-1} as CO_2 (Raymond *et al.*, 2013) and 0.65 Pg C yr^{-1} as CH_4 (Bastviken *et al.*, 2011).

Global estimates of CH_4 release from rivers are on the order of 1.5 Tg CH_4 yr^{-1} (Bastviken *et al.*, 2011). However, due to the scarcity of river CH_4 data this estimate was based on a small number of studies, largely from temperate areas. The lack of data from tropical rivers is particularly important given their large area and higher rate of emissions per unit area compared to temperate ecosystems (Bastviken *et al.*, 2011).

Most of the previous CH_4 flux measurements in the Amazon were done in the adjacent areas of the river channel, such as the floodplains locally called “varzeas”, lakes and flooded forest (Bartlett *et al.*, 1988, Belger *et al.*, 2011, Crill *et al.*, 1988, Devol *et al.*, 1988, Devol *et al.*, 1990, Rosenqvist *et al.*, 2002) or in hydroelectric (Abril *et al.*, 2005, Kemenes *et al.*, 2007, Lima, 2005).

However, the large concentration of CH_4 found in the Amazon river channel (Richey *et al.*, 1988) have shown the potential importance of this river itself as a source of CH_4 to the atmosphere. Significant CH_4 fluxes from three other tropical rivers were recently estimated in Africa (Kone *et al.*, 2010). However, these studies focused only on the diffusive component of CH_4 fluxes, calculated from water-air CH_4 concentration gradient and piston velocity, whereas recent studies have shown that ebullition can also be important

in running waters (Baulch *et al.*, 2011). Therefore, studies on CH_4 emissions demand the evaluation of both ebullition and diffusive components.

Here we present the results from total flux measurements separated into diffusive and ebullitive components in the Amazon River and most of its main tributaries (Solimões, Negro, Madeira, Tapajós and Xingu Rivers), as well as their general spatial and temporal distribution. Our data points to a more significant role of the Amazon basin in the global CH_4 budget than previously estimated.

Methods

Sites description and sampling scheme

The Amazon river basin stands out as the largest river system on Earth (Archer, 2005), formed by an extensive network of tributaries draining approximately 6 million km² of Andean and lowland basins that feed the 6,700 km long main river channel (Richey *et al.*, 1988). In general, the weather is characterized by high temperatures with low variations throughout the year and is divided into well defined wet and dry seasons. Precipitation has strong seasonality modulated by shifts in the Intertropical Convergence Zone (ITCZ). The southward shift of the ITCZ during austral summer brings a large amounts of moisture to the basin, generating a monsoon precipitation system (Grimm *et al.*, 2005, Vera *et al.*, 2006), which results in large variations in river water levels.

The Amazon river tributaries have distinct characteristics related to their water types and channel morphology. A general classification by water color is frequently used to separate rivers in the Amazon Basin (Sioli, 1985). Black water rivers such as Negro River usually drain lowland areas with heavily weathered rocks and sandy soils and have high dissolved organic matter content, low amounts of suspended sediments, median turbidity, low ionic strength, and high acidity (Mayorga & Aufdenkampe, 2002, Sioli, 1985). White water rivers such as Solimões and Madeira Rivers have their upstream catchment draining Andean areas and have high suspended sediment loads and dissolved solids concentrations, with neutral to alkaline pH (Mayorga & Aufdenkampe, 2002, Sioli, 1985). Clear water rivers such as Tapajós and Xingu drain the Brazilian shield and have low suspended

sediment loads, intermediary ionic content and slightly alkaline pH (Mayorga & Aufdenkampe, 2002, Sioli, 1985).

Amazonian rivers have different types of depositional systems with varied sedimentary dynamics and sediment distribution (Archer, 2005, Latrubesse *et al.*, 2005). This heterogeneity in sedimentary dynamics is seen in the occurrence of channel areas with higher deposition of organic rich sediment where CH_4 production is favored. Great differences in channel morphology and sediment deposition occur downstream from our studied site in some tributaries, as observed during field trips for CH_4 measurements. The mouths of the Negro, Xingu and Tapajós Rivers are blocked by sediment bars from the Amazon main channel. This damming of the lower portion of these tributaries generates wide channels (up to 19 km wide) with low water flow and regular wave action, promoting lake-like sedimentary dynamics in which deposition of organic rich mud in the central portion of the channel is common. Rivers draining highlands in the Andes such as the Solimões and Madeira have high suspended sediment load and their lowermost reaches are characterized by relatively narrow (1.5-3.5 km wide) and straight channels dominated by sand deposition with mud deposition occurring mainly over adjacent floodplains. The Amazon main channel has these same characteristics upstream from the Xingu River mouth. The Xingu River has an unique channel morphology. Its upstream sectors drain bedrock from an incised valley and have relatively low sediment deposition rates due to high water flow. This is in contrast with its depositional lake-like river mouth.

Concentrations and fluxes (total flux, diffusive flux, and ebullition) of CH_4 to the atmosphere were measured on 52 occasions at 34 sites at the Negro, Solimões, Preto da Eva, Madeira, Tapajós, Xingu, Pará and Amazon Rivers and at a white water lake (Lake Curuai) in the Amazon River floodplain. Sixteen of these sites were measured during both

high (May 2012) and low (November 2012) water seasons and one site at Tapajós River was also measured in the falling water season (July 2012) (site number 14 in Figure 1). The remaining sites were visited only once during low, high or falling water season (see Table 1 for details). Sites in the Amazon River, near Óbidos, (numbered 27, 28 and 29 in Figure 1 and Table 1) and sites in the Pará River near Belém (numbered 23, 24 and 25) represents two cross-section profiles where measurements were made at three locations equally spaced across the channel of those rivers. Figure 1 and Table 1 show details about sampling periods and additional information about the sites.

CH_4 flux measurements

Surface water samples were collected simultaneously with flux measurements. CH_4 concentrations in water were determined after headspace extraction according to the methods of Bastviken et al. (2010). Dissolved CH_4 concentration was calculated using Henry's Law adjusted for temperature according to Wiesenburg and Guinasso (1979) following analysis in a Shimadzu GC17A gas chromatograph, modified to contain an online methanizer coupled to a FID detector.

Chamber deployments for CH_4 total flux at all sites were performed in the center of the river channels using floating chambers as described by Bastviken et al. (2010). Measurements were made for approximately one hour at each site while drifting, using 7 to 15 chambers separated 1.5 m from each other. The chambers used were of the same type as previously tested and shown to produce non-biased flux values relative to other flux measurement methods (Cole *et al.*, 2010, Galfalk *et al.*, 2013). Using many chambers simultaneously increases the probability of capturing ebullition and allows for the

calculation of diffusive flux and ebullition. Total flux and the contribution from diffusive and ebullitive emissions were calculated according to Bastviken et al. (2004, 2010). Samples from chambers were withdrawn using syringes and immediately transferred to 20 ml glass vials filled with salt solution to prevent solubility and capped with a 10 mm thick butyl rubber stopper and an aluminum crimp seal. Gas concentrations were measured by gas chromatography as above. Air temperature, atmospheric pressure and wind speed were measured with a weather station (HOBO; Onset Computer Corporation, Bourne, MA, USA) installed on the boat and water temperature was measured with a pH meter (Orion 290APlus; Thermo Fisher Scientific Inc., Waltham, MA, USA). Flux measurements were done with wind speed ranging from 0.36 to 6 m/s.

Diffusive flux calculations

Diffusive flux across the water surface into the floating chamber can be described by the equation:

$$F = k \cdot (C_w - C_{fc}), \qquad (1)$$

where F is flux (mol $m^{-2}d^{-1}$), k the piston velocity (m d^{-1}), C_w is the concentration of CH_4 measured in the water (mol m^{-3}), and C_{fc} is the CH_4 concentration in the water at equilibrium with the CH_4 partial pressure in the floating chamber (Cole & Caraco, 1998). However, in equation (1) the flux is partially driven by the change in concentration, which will decrease with time in the chambers as the internal concentration increase. Therefore, this simple calculation will underestimate the instantaneous flux rate. In order to reduce this error, we solved for k to estimate instantaneous flux (e.g. the flux for each time step; here time zero (0) to time "t", $F_{0\text{-}t}$. First, F is expressed as

$$F_{0-t} = \frac{(n_t - n_0)}{A} \qquad (2),$$

where n_0 and n_t are the number of moles in the chamber at time zero and time "t" and A is the chamber area. Then, the moles are expressed as P_0 and Pt given conversion according to the common gas law ($PV=nRT$). Finally, the concentration numbers are also expressed as corresponding gas pressure following Henrys Law ($C=K_hP$). Hence, by making this equation continuous, instead of having discrete time steps (e.g. dP/dt instead of P_t-P_0), Equation (1) could be rewritten as:

$$\left(\frac{dP}{dt}\right) \cdot \left(\frac{V}{R \cdot T \cdot A}\right) = k \cdot (K_h \cdot P_w - K_h.P_0), \qquad (3)$$

where dP/dt is the slope of CH_4 accumulation in the chamber (Pa d^{-1}), V is the chamber volume (m^3), R is the gas constant (8.314 m^3 Pa $K^{-1}mol^{-1}$), T is temperature (K), P_w is the partial pressure of CH_4 in the chamber at equilibrium with C_w (Pa), P_0 is the partial pressure of CH_4 in the chamber at time 0 (approximately the same than atmosphere), and K_h is the Henry's Law constant for CH_4 (mol m^{-3} Pa^{-1}). Thus,

$$k = \left(\frac{dP}{dt}\right) \cdot \frac{V \cdot (P_w - P_0)}{K_h \cdot R \cdot T \cdot A} \qquad (4)$$

After solving for k using equations 4 the instantaneous flux was calculated using equation (1). The temperature dependence of K_h was calculated from the Bunsen coefficients given by Wiesenburg and Guinasso (1979).

Ebullition calculations

To determine which chambers captured ebullition we used the distributions and variance of the apparent piston velocities as described in Bastviken *et al*. (2004, 2010). First the calculated (apparent) k values for each chamber were transformed into k_{600} values,

allowing k values to be compared for any gas and temperature (Jahne *et al.*, 1987, Wanninkhof, 1992). Ebullition makes calculated apparent k_{600} values substantially higher than those receiving CH_4 only by diffusive flux, allowing the separation of the two flux components. In each measurement, the apparent k_{600} of each chamber was divided by the minimum k_{600} found in the same set of chambers, which we attributed solely to diffusive flux. Moreover, in a given area and time, the diffusive flux has a constant rate. Thus, chambers receiving only diffusive flux would have similar and lower flux rates and could be distinguished from the chambers receiving ebullition. However, in one site all chambers displayed a large discrepancy in flux rates, indicating that all chambers could have received ebullition. In this case, as the lowest value was similar with the diffusion measured in nearby sites, we considered that value as diffusion. The frequency distribution of this ratio (k_{600} / minimun k_{600}) for all chambers clearly indicated two distinct groups of ratios, one between 0.99–2.0 and another >2 (Figure 2). For this reason a ratio of 2 was chosen as threshold for significant inputs of CH_4 into the chamber by ebullition. For the chambers that received ebullition flux we first calculated the diffusive flux from equation (1) using the site averaged k_{600} from the other chambers which received diffusive flux only, with the remaining CH_4 flux into the chambers attributed to ebullition only. For comparison among rivers, ebullition was normalized to the area covered by all chambers, including the chambers that did not receive ebullition, which were computed as 0 for average calculations.

Classification of Sediment

Most of the sites were surveyed for sediment type using a Van Veen grab sampler. Sediment types were divided into four general groups: mud, sand, a mixture of fine sand with mud and non-identified. The non-identified groups consisted of sites where we were not able to sample due to depth or malfunctioning of the grab sampler. However, water flow regime at these sites was similar to areas with sand or sand-mud sediments. Water depth was measured using a sonar (Garmin GPSMAP 521s; Garmin Ltd, Olathe, KS, USA).

Spatiotemporal statistical analysis

To understand the spatial and temporal CH_4 flux variability we performed a series of comparisons including: (1) difference in CH_4 fluxes within the same river; (2) differences in CH_4 fluxes between rivers; (3) differences in CH_4 fluxes for areas with different sediment types; (4) differences in CH_4 fluxes between water types and (5) seasonal variations in CH_4 fluxes. To obtain a more robust analysis in the seasonal comparison we used only data from sites that were measured in both low and high water seasons. Analysis of variance (ANOVA) followed by Tukey post-hoc tests with log transformed data were used to check for differences between comparisons. A non-parametric statistic was necessary for ebullition due to the non-normal distribution, even after log transformations. For that purpose we choose Kruskal-Wallis to test the influence of sediment type and depth on ebullition. All statistics were done using each chamber and deployment period as one independent measurement.

Upscaling

The surface area covered by rivers in the Amazon basin was obtained from the water class of the South America land cover map (Brown *et al.*, 2003). In this map only rivers wider than 200 m were mapped, and since our measurements were done only in rivers wider than 1km we decided not to consider rivers smaller than 200m in our extrapolation. Further measurements in smaller rivers and streams are still needed to better constrain CH_4 flux from riverine systems in the Amazon. Lakes in the floodplain of the Amazon River were removed while large depositional areas (lake-like) within channels included.

For a more precise upscaling of CH_4 flux from rivers of the Amazon basin, we calculated each river flux rate separately and summed them to obtain whole basin estimates. For those rivers where different CH_4 fluxes were identified in lake-like areas and straight fluvial channels, mean flux rates for these reaches were calculated separately. Seasonal average CH_4 fluxes for low and high water seasons (each corresponding to a time period of six months) were calculated separately and then summed to compose the annual CH_4 flux rate. The extrapolation to other large rivers in the Amazon basin that were not measured was done using the average from all rivers. Flux ranges for each river were calculated based on the average of the standard errors of the means.

Results

An overview of the results is presented in Table 2. Dissolved CH_4 concentrations ranged from 0.02 to 0.5 µM, with average total fluxes of 0.01 to 40.3 mmol CH_4 m^{-2} d^{-1} and an overall average, excluding Curuai Lake, of 1.4 mmol CH_4 m^{-2} d^{-1}. Diffusive fluxes accounted for 66 % of total emissions, with a range of single measurements from 0.01 to 18.6 mmol CH_4 m^{-2} d^{-1}, while the remaining 34% attributed to ebullition ranged from 0.2 to 35.7 mmol CH_4 m^{-2} d^{-1} (Table 2). Ebullition was captured by at least one of the chambers in 36 % of the measurements and when registered, its contributions varied from 5 to 83 % of the total flux in a single measurement.

Flux variability within rivers

To test for spatial variability in CH_4 flux within rivers we analyzed the longitudinal and cross-channel differences among sites within the same river. The cross-channel profiles were done in two locations, one in the Amazon and another in the Pará River. Due to limited replication for each specific site within each river for this comparison we used only the diffusive flux component. Ebullition is discussed in other comparisons below. A One-way ANOVA followed by a Tukey post-hoc test ($p<0.05$) showed that at the river scale, diffusive fluxes were different in both longitudinal and cross-channel comparisons in all rivers. Fluxes in the Negro, Solimões and Madeira Rivers increased downstream. If we exclude estuarine sites in the Amazon River the same downstream increase was observed. The Tapajós River had an opposite pattern and the Xingu River had no clear spatial pattern (Figure 3). The cross-channel trends varied between the two rivers considered with higher

fluxes in the center of the Amazon but an increasing trend from north to south banks of the Pará River (Figure 4).

River bed sediments influence on total flux

The influence of riverbed sediment type on total CH_4 flux was tested by comparing emissions from locations with varying sediment type. The two end members are represented by sand substrate from channels with high water flow and mud substrate from wide channels with low water flow and deposition of suspended sediments. A mixed sand-mud substrate was also considered. Using log transformed data, we observed significant differences in total flux comparing sites with different types of sediment (ANOVA, p-value < 0.001) (Figure 5A). Significantly higher total fluxes were observed in sites with mud in riverbed sediments (Table 3). Average fluxes for non-identified, sand/mud mixture, and sand sediments were all lower and similar in magnitude (Table 3).

Flux variability among rivers and water type

We observed a wide range of total CH_4 fluxes among rivers with averages ranging from 0.04 mmol m^{-2} d^{-1} in Madeira River to 6.0 mmol m^{-2} d^{-1} in Xingu River (more details in Table 2). Significant differences among rivers were tested using ANOVA test (*p*-value < 0.001), followed by Tukey post-hoc (Figure 5B). The Xingu River had the highest total flux and was different from all other rivers. Average Xingu River emissions per m^2 were 2-100 fold larger than corresponding emissions from the other rivers (Table 2). Tapajós and Amazon Rivers presented the second and third highest CH_4 emissions, with an average total

flux of 2.4 and 1.3 mmol m^{-2} d^{-1}, respectively. These three highest river fluxes were all similar to, or higher than, our flux measurements at Lake Curuai (mean = 1.1 mmol m^{-2} d^{-1}). The Madeira River had the lowest flux among all measured rivers (Table 2).

Clear water rivers had significantly higher total fluxes (mean= 4.6 mmol m^{-2} d^{-1}), while white and black water rivers were statistically similar , with mean fluxes of 0.7 and 0.4 mmol m^{-2} d^{-1}, respectively (ANOVA, $p < 0.001$; Figure 5C, Table 3).

Seasonal variability

Since most of the sites measured during the falling water season were visited only on one occasion, they were not considered for this test. Here we choose only data from the 16 sites that were measured during low and high water seasons (Figure 1, Table 1). An overall analysis comparing all measurements done in low and high water seasons shows significantly higher emissions during low water (4.1 versus 0.9 mmol m^{-2} d^{-1}; ANOVA, $p < 0.001$; Figure 5D, Table 3). Considering seasonal variability for each river separately, all rivers had higher median fluxes during low water (Figure 6). However, statistically significant seasonal differences were only observed for Tapajós and Xingu Rivers (two-way ANOVA, *p*-value = 0,025).

Ebullition

In most rivers diffusion was the main component of CH_4 emission. However, our results show that more than 50% of the total CH_4 released by the Xingu River to the

atmosphere can be attributed to ebullition. Ebullition was also registered in the Amazon, Tapajós, Negro, Pará and Solimões Rivers, but in lower proportions (Figure 7, Table 2).

The highest rates of ebullition were measured in sites with mud substrate between 10 and 20 m water depth (Figure 8A). A Kruskal-Wallis test was used to confirm the difference in ebullition according to sediments types (n = 37, p = 0.029). The influence of water depth was also observed (Figure 8), with significantly higher ebullition during the low water season (Kruskal-Wallis, n = 37, p = 0.026).

Whole basin CH_4 emission from large rivers

The calculated surface area covered by rivers wider than 200m in the Amazon basin was 91,212 km^2. Flux rates were calculated separately for each tributary basin and then summed. Tapajos and Xingu Rivers presented significant difference in flux rates among seasons. Thus, an average for each season in each river was calculated and used for the river basin extrapolation. Additionally, for the Xingu basin extrapolation a seasonal average considering sites with mud was calculated separately from those with sand. This allowed a more precise extrapolation of the CH_4 flux for large rivers in the whole Amazon basin, resulting in a mean flux of 0.49 Tg CH_4 yr^{-1}, with a range calculated based on the standard error of the mean from 0.40 to 0.58 Tg CH_4 yr^{-1}.

Discussion

In the present study we found higher CH_4 fluxes than previously reported. We believe that this is the result of our use of the multiple floating chambers approach for measuring CH_4 emission from rivers and due to the inclusion of the major tributaries of the Amazon River, which increased the variability of river environments measured. The use of chambers and the several different rivers sampled enabled us to find hotspots where ebullition was very significant. Thus, capturing larger number of events with ebullitive fluxes could result in an even larger contribution of the Amazon in the CH_4 global cycle than reported here.

Comparison with previous estimates

Previous studies in the Amazonian rivers, which only used dissolved measurements to calculate diffusive emission of CH_4 (Bartlett *et al.*, 1988, Richey *et al.*, 1988), were significantly lower than our estimates using chambers and including ebullition. The previous Solimões/Amazon River channel CH_4 flux ranged from 0.17 to 0.23 mmol m^{-2} d^{-1} (Bartlett *et al.*, 1988, Richey *et al.*, 1988). Including mean CH_4 flux from the tributaries expanded the range for Amazonian river from 0.04 to 6.0 mmol CH_4 m^{-2} d^{-1}, found in the Madeira and Xingu Rivers, respectivley. Comparing only our sites within the same Solimões/Amazon River stretch we observed fluxes that were approximately twice as high as previous measurements. The use of floating chambers, when properly designed, is an efficient way to calculate *k* and determine fluxes (Cole *et al.*, 2010, Galfalk *et al.*, 2013). Thus our result is more realistic than simulating fluxes from dissolved CH_4 concentrations

due to the effective calculation of *k* and inclusion of ebullitive fluxes, which was overlooked previously in the relatively few studies that currently exist.

Spatiotemporal CH_4 flux heterogeneity

Our results showed a trend of increasing fluxes downriver in Negro, Solimões, Madeira and Amazon Rivers. It is possible that the downstream flux increase could be influenced by a combination of factors such as CH_4 concentration, and higher water turbulence caused by the confluence with another large river. This increasing trend in CH_4 emissions downriver was also observed in the Yukon River and its tributaries (Striegl *et al.*, 2012), but no further discussion regarding the causes was given.

Cross-channel profiles of dissolved CH_4 in five locations of the Amazon River done by Richey *et al.* (1988) showed lower concentrations in the center compared to the banks. This is in agreement with patterns observed in lakes (Hofmann, 2013, Schilder *et al.*, 2013). While our concentration results follow a similar trend to that of the Richey *et al.* (1988) data, the diffusive flux patterns we found are opposite in magnitude to the concentration trend with highest fluxes in the center of the channel (Figure 4a). Flux and concentration profiles in the Pará River followed the same pattern, increasing from the north to the south bank (Figure 4b). In both these rivers, there was a large tributary several kilometers upstream entering at the same channel side where our profiles showed higher dissolved CH_4, indicating that the concentrations could be influenced by incomplete mixing and transport from tributaries upriver, as suggested by Bartlett *et al*. (1990). The local diffusive flux patterns result from a combination of concentration and water turbulence. The latter

could be attributed to depth, water and wind speed in the river channel increasing the gas exchange coefficient.

Sites with mud sediments had higher total flux rates to the atmosphere than areas with mixtures of mud/sand or just sand. These mud sediment sites had flux rates even higher than observed in open water of lakes from the Amazon River floodplain (1.7 mmol m^{-2} d^{-1}) (Bartlett *et al.*, 1988, Crill *et al.*, 1988) and similar to fluxes in reservoirs (0.9 – 5.2 mmol m^{-2} d^{-1}; Tucurui, Samuel and Balbina (Lima, 2005). These low water-speed areas which accumulate fine grained sediments rich in organic matter can function as local hotspots of CH_4 production within the channel and could be used as a predictor of future CH_4 hotspots in planned hydroelectric reservoirs in the Amazon basin.

Our results indicate higher total and diffusive fluxes in clear water rivers (Xingu and Tapajós) (Table 3 and Figure 5). M. F. F. L. Rasera (unpublished data) also found higher diffusive fluxes in clear water rivers (Araguaia, Javaés and Teles Pires) than in the Negro and Solimões Rivers, which represent respectively, black and white water river types. Despite the dominance of mud in our clear water sites, sand areas had similar fluxes, and both sediment types exhibited higher fluxes than those in black and white water sites. Clear water rivers are characterized by high level of dissolved oxygen and light penetration, both potentially inhibitory factors for methanotrophic bacteria activity (Dumestre *et al.*, 1999, Rudd *et al.*, 1976), which could indicate that in these rivers there is less methane oxidation in the water column. A further indicative of lower oxidation rates in studied clear water rivers is the more depleted isotopic signature ^{13}C-CH_4 in surface water than in black and white water rivers (H. O. Sawakuchi, unpublished data).

In regards to seasonal patterns in CH_4 fluxes, our measurements showed significantly higher fluxes during the low water season. The same pattern was observed in

tropical rivers in Africa (Kone *et al.*, 2010) and temperate European rivers (Middelburg *et al.*, 2002). These higher fluxes during low water season in Amazonian rivers indicate that adjacent flooded areas may not be as important sources of CH_4 to the river channel as suspected previously (Bartlett *et al.*, 1990, Devol *et al.*, 1990, Richey *et al.*, 1988). This pattern may be explained by the greater dilution of incoming CH_4 from sediments and ground waters and greater time for CH_4 oxidation in deeper water columns during high water periods. Both effects could contribute to the lower values observed during high water season. Furthermore, we registered most of the ebullition in depths between 10 and 20 m in areas where CH_4 is produced within the channel. At these areas, the increase in hydrostatic pressure during high water season resulted in significantly lower ebullition. These changes in hydrostatic pressure and CH_4 release through ebullition were also observed in a tidally influenced estuary in North Caroline (Martens & Val Klump, 1984), and are common in lakes (Ostrovsky *et al.*, 2008, Wik *et al.*, 2013).

Role of ebullition in Amazonian rivers

Even though measurements were done mostly in the middle of the channel, ebullition was detected in all sorts of sediments, including areas with sand, and was an important pathway of CH_4 emission. Thermogenic, geological sources of CH_4 in ebullition cannot be excluded but seem unlikely. It is more likely that the ebullition in sites with sand on the bottom is driven by the degradation of buried layers below the sand with a higher content of organic matter. This was directly observed in a shallow area near the channel margin of the Xingu River, where a bank of leaves was buried below about 25 cm of coarse sand and a large amount of bubbles was being released. Ebullitive fluxes in stream and

rivers can be responsible for 10% to 80% of the CH_4 transport and seem positively related with the proportion of clay and silt in the bed sediment (Baulch *et al.*, 2011).

CH_4 flux from Amazonian rivers in the global scenario

We estimate an emission of CH_4 from large rivers in the Amazon Basin of 0.49 Tg CH_4 yr^{-1} (standard error ± 0.09 Tg CH_4 yr^{-1}). This mean value represents approximately 1.7 % of the estimated emissions from wetlands in Amazon (Melack *et al.*, 2004). Our estimate accounting for large rivers only in the Amazon basin, corresponds to 12.5 % of this amount. Compared to the CH_4 fluxes from rivers estimated by Bastviken *et al*. (2011), the Amazonian rivers contribute with 44 - 65 % of the global tropical river emissions, and 22-28% of the global river emission. Using the same tropical and global river areas as in Bastviken et al. (2011), 176,856 km^2 and 357,627 km^2, respectively, and our average value of CH_4 flux from Amazonian rivers, we compute a new tropical river emission estimate ranging from 1.18 - 1.66 Tg CH_4 yr^{-1} which is to 31 – 84 % higher than the previous estimate done by Bastviken et al. (2011) using temperate rivers as reference. Our global estimate ranges from 1.78 to 2.26 Tg CH_4 yr^{-1} which is 19-51 % higher than the previous 1.5 Tg CH_4 yr^{-1} estimated by Bastviken et al. (2011).

Our study shows a high heterogeneity in CH_4 flux across spatial and temporal scales from large rivers in the Amazon Basin. At the river scale, local characteristics, such as CH_4 concentration and water turbulence, could lead to different fluxes rates along the river and across the channel. Furthermore, geomorphologic features can drive different patterns of sediment deposition within river channels, creating hotspots of CH_4 production with high ebullitive fluxes. At the basin scale, geologic formations of the basin terrain will have an

important influence on the water type, which in turn, can influence emission through oxidation. Despite the spatial difference within rivers, there is still a clear seasonal signal in CH4 emissions. Therefore, all this variability in CH_4 fluxes from rivers should be addressed and considered for extrapolations.

The CH_4 emission rates estimated here put the large Amazonian rivers in the context of global CH_4 sources. As we observed, tropical rivers have higher emission than temperate rivers. However, specific and more detailed studies in small rivers and streams in the Amazon Basin and in other tropical rivers were not included in this study and are still needed. More importantly, we have shown that future flux measurements in rivers should be designed to use multiple floating chambers to cover not only diffusive flux but also ebullition. More studies are needed to better understand the high variability of fluxes of CH_4 within rivers and more accurate CH_4 budgets, including sources and sinks, are still needed to better constrain global river emissions of CH_4.

Acknowledgments

This study was supported by FAPESP, Grants 08/58089-9, 2011/06609-1, 2011/14502-2 and 2012/17359-9, for financial support and scholarship. We thank Alexandra Montebello and Maria de Fátima F. L. Rasera for assistance in the laboratory; Hillândia B. da Cunha, Ingo Wahnfried, José Mauro S. Moura, Carlos Henrique Grohmann, Tatiana S. Pereira, Daímio C. Brito, Alan C. Cunha and all people assisted in field work and Will Gagne-Maynard and two anonymous reviewers for their constructive comments to the manuscript.

References

Abril G, Guerin F, Richard S *et al.* (2005) Carbon dioxide and methane emissions and the carbon budget of a 10-year old tropical reservoir (Petit Saut, French Guiana). *Global Biogeochemical Cycles,* **19**.

Archer Aw (2005) Review of Amazonian Depositional Systems. In: *Fluvial Sedimentology VII.* (ed Blum M Ms, Leclair S) pp Page., Blackwell Publishing Ltd.

Bartlett Kb, Crill Pm, Bonassi Ja, Richey Je, Harriss Rc (1990) Methane flux from the Amazon River floodplain - emission during rising water. *Journal of Geophysical Research-Atmospheres,* **95**, 16773-16788.

Bartlett Kb, Crill Pm, Sebacher Di, Harriss Rc, Wilson Jo, Melack Jm (1988) Methane flux from the central amazonian floodplain. *Journal of Geophysical Research-Atmospheres,* **93**, 1571-1582.

Bastviken D, Cole J, Pace M, Tranvik L (2004) Methane emissions from lakes: Dependence of lake characteristics, two regional assessments, and a global estimate. *Global Biogeochemical Cycles,* **18**, Gb4009.

Bastviken D, Santoro Al, Marotta H, Pinho Lq, Calheiros Df, Crill P, Enrich-Prast A (2010) Methane Emissions from Pantanal, South America, during the Low Water Season: Toward More Comprehensive Sampling. *Environmental Science & Technology,* **44**, 5450-5455.

Bastviken D, Tranvik Lj, Downing Ja, Crill Pm, Enrich-Prast A (2011) Freshwater Methane Emissions Offset the Continental Carbon Sink. *Science,* **331**.

Battin Tj, Luyssaert S, Kaplan La, Aufdenkampe Ak, Richter A, Tranvik Lj (2009) The boundless carbon cycle. *Nature Geoscience,* **2**, 598-600.

Baulch Hm, Dillon Pj, Maranger R, Schiff Sl (2011) Diffusive and ebullitive transport of methane and nitrous oxide from streams: Are bubble-mediated fluxes important? *Journal of Geophysical Research-Biogeosciences,* **116**, G04028.

Belger L, Forsberg Br, Melack Jm (2011) Carbon dioxide and methane emissions from interfluvial wetlands in the upper Negro River basin, Brazil. *Biogeochemistry,* **105**, 171-183.

Brown J, Loveland T, Ohlen D, Zhu Z (2003) LBA Regional Land Cover from AVHRR, 1-km, Version 1.2 (IGBP). *Available on-line [http://daac.ornl.gov] from Oak Ridge National Laboratory Distributed Active Archive Center, Oak Ridge, Tennessee, U.S.A. doi:10.3334/ORNLDAAC/679*.

Cole Jj, Bade Dl, Bastviken D, Pace Ml, Van De Bogert M (2010) Multiple approaches to estimating air-water gas exchange in small lakes. *Limnology and Oceanography-Methods,* **8**, 285-293.

Cole Jj, Caraco Nf (1998) Atmospheric exchange of carbon dioxide in a low-wind oligotrophic lake measured by the addition of SF6. *Limnology and Oceanography,* **43**, 647-656.

Cole Jj, Prairie Yt, Caraco Nf *et al.* (2007) Plumbing the global carbon cycle: Integrating inland waters into the terrestrial carbon budget. *Ecosystems,* **10**, 171-184.

Crill Pm, Bartlett Kb, Wilson Jo *et al.* (1988) Tropospheric methane from an amazonian floodplain lake. *Journal of Geophysical Research-Atmospheres,* **93**, 1564-1570.

Devol Ah, Richey Je, Clark Wa, King Sl, Martinelli La (1988) Methane emissions to the troposphere from the Amazon floodplain. *Journal of Geophysical Research-Atmospheres,* **93**, 1583-1592.

Devol Ah, Richey Je, Forsberg Br, Martinelli La (1990) Seasonal dynamics in methane emission from the amazon River floodplain to the troposphere. *Journal of Geophysical Research-Atmospheres,* **95**, 16417-16426.

Dumestre Jf, Guezennec J, Galy-Lacaux C, Delmas R, Richard S, Labroue L (1999) Influence of light intensity on methanotrophic bacterial activity in Petit Saut Reservoir, French Guiana. *Applied and Environmental Microbiology,* **65**, 534-539.

Galfalk M, Bastviken D, Fredriksson S, Arneborg L (2013) Determination of the piston velocity for water-air interfaces using flux chambers, acoustic Doppler velocimetry, and IR imaging of the water surface. *Journal of Geophysical Research-Biogeosciences,* **118**, 770-782.

Grimm Am, Vera Cs, Mechoso Cr (2005) The South American Monsoon System. *The Global Monsoon System: Research and Forecast*, 219-238.

Hofmann H (2013) Spatiotemporal distribution patterns of dissolved methane in lakes: How accurate are the current estimations of the diffusive flux path? *Geophysical Research Letters,* **40**, 2779-2784.

Jahne B, Munnich Ko, Bosinger R, Dutzi A, Huber W, Libner P (1987) On the parameters influencing air-water gas exchange. *Journal of Geophysical Research-Oceans,* **92**, 1937-1949.

Kemenes A, Forsberg Br, Melack Jm (2007) Methane release below a tropical hydroelectric dam. *Geophysical Research Letters,* **34**.

Kone Yjm, Abril G, Delille B, Borges Av (2010) Seasonal variability of methane in the rivers and lagoons of Ivory Coast (West Africa). *Biogeochemistry,* **100**, 21-37.

Latrubesse Em, Stevaux Jc, Sinha R (2005) Tropical rivers. *Geomorphology,* **70**, 187-206.

Lima Ibt (2005) Biogeochemical distinction of methane releases from two Amazon hydroreservoirs. *Chemosphere,* **59**, 1697-1702.

Martens Cs, Val Klump J (1984) Biogeochemical cycling in an organic-rich coastal marine basin 4. An organic carbon budget for sediments dominated by sulfate reduction and methanogenesis. *Geochimica et Cosmochimica Acta,* **48**, 1987-2004.

Mayorga E, Aufdenkampe Ak (2002) Processing of bioactive elements in the amazon river system. In: *The ecohydrology of south american rivers and wetlands.* (ed Mcclain Me) pp Page. Oxfordshire, IAHS Press.

Melack Jm, Hess Ll, Gastil M, Forsberg Br, Hamilton Sk, Lima Ibt, Novo E (2004) Regionalization of methane emissions in the Amazon Basin with microwave remote sensing. *Global Change Biology,* **10**, 530-544.

Middelburg Jj, Nieuwenhuize J, Iversen N *et al.* (2002) Methane distribution in European tidal estuaries. *Biogeochemistry,* **59**, 95-119.

Ostrovsky I, Mcginnis Df, Lapidus L, Eckert W (2008) Quantifying gas ebullition with echosounder: the role of methane transport by bubbles in a medium-sized lake. *Limnology and Oceanography-Methods,* **6**, 105-118.

Raymond Pa, Hartmann J, Lauerwald R *et al.* (2013) Global carbon dioxide emissions from inland waters. *Nature,* **503**, 355-359.

Richey Je, Devol Ah, Wofsy Sc, Victoria R, Riberio Mng (1988) Biogenic gases and the oxidation and reduction of carbon in Amazon river and floodplain waters. *Limnology and Oceanography,* **33**, 551-561.

Richey Je, Melack Jm, Aufdenkampe Ak, Ballester Vm, Hess Ll (2002) Outgassing from Amazonian rivers and wetlands as a large tropical source of atmospheric CO2. *Nature,* **416**, 617-620.

Rosenqvist A, Forsberg Br, Pimentel T, Rauste Ya, Richey Je (2002) The use of spaceborne radar data to model inundation patterns and trace gas emissions in the central Amazon floodplain. *International Journal of Remote Sensing,* **23**, 1303-1328.

Rudd Jwm, Furutani A, Flett Rj, Hamilton Rd (1976) Factors controlling methane oxidation in Shield Lakes: The role of nitrogen fixation and oxygen concentration. *Limnology and Oceanography,* **21**, 357-364.

Schilder J, Bastviken D, Van Hardenbroek M, Kankaala P, Rinta P, Stoetter T, Heiri O (2013) Spatial heterogeneity and lake morphology affect diffusive greenhouse gas emission estimates of lakes. *Geophysical Research Letters,* **40**, 5752-5756.

Sioli H (1985) *Amazônia: Fundamentos de ecologia da maior região de florestas tropicais,* Petrópolis, Editora Vozes.

Striegl Rg, Dornblaser Mm, Mcdonald Cp, Rover Jr, Stets Eg (2012) Carbon dioxide and methane emissions from the Yukon River system. *Global Biogeochemical Cycles,* **26**, GB0E05.

Tranvik Lj, Downing Ja, Cotner Jb *et al.* (2009) Lakes and reservoirs as regulators of carbon cycling and climate. *Limnology and Oceanography,* **54**, 2298-2314.

Vera C, Higgins W, Amador J *et al.* (2006) Toward a unified view of the American Monsoon Systems. *Journal of Climate,* **19**, 4977-5000.

Wanninkhof R (1992) Relationship betwenn wind-speed and gas-exchange over the ocean. *Journal of Geophysical Research-Oceans,* **97**, 7373-7382.

Wiesenburg Da, Guinasso Nl (1979) Equilibrium solubilities of methane, carbon-monoxide, and hydrogen in water and sea-water. *Journal of Chemical and Engineering Data,* **24**, 356-360.

Wik M, Crill Pm, Varner Rk, Bastviken D (2013) Multiyear measurements of ebullitive methane flux from three subarctic lakes. *Journal of Geophysical Research: Biogeosciences,* **118**, 1307-1321.

Table 1. Additional information about sampling sites showed in Figure 1.

Location no[a]	River	Sediment	Water type	Sedimentary dynamics	Water seasons [b]		
					Low	High	Falling
1	Negro	Sand/Mud	Black	Lake-like	x	x	-
2	Negro	Sand	Black	Lake-like	x	x	-
3	Negro	Sand/Mud	Black	Lake-like	x	x	-
4	Solimões	Sand	White	Straight fluvial channel	x	x	-
5	Solimões	Sand	White	Straight fluvial channel	x	x	-
6	Solimões	Sand	White	Straight fluvial channel	x	x	-
7	Preto da Eva	Mud	Black	Lake-like	-	x	-
8	Madeira	Sand	White	Straight fluvial channel	-	x	-
9	Madeira	Sand	White	Straight fluvial channel	-	x	-
10	Madeira	Sand	White	Straight fluvial channel	-	x	-
11	Lake Curuai	Mud	White	Floodplain lake	-	-	x
12	Tapajós	Mud	Clear	Straight channel	x	-	-
13	Tapajós	Mud	Clear	Lake-like	x	x	-
14	Tapajós	Mud	Clear	Lake-like	x	x	x
15	Tapajós	Mud	Clear	Lake-like	x	x	-
16	Xingu	Sand	Clear	Rapids-waterfalls	x	x	-
17	Xingu	Sand	Clear	Rapids-waterfalls	x	x	-
18	Xingu	Sand	Clear	Lake-like	x	x	-
19	Xingu	Mud	Clear	Lake-like	x	x	-
20	Xingu	Mud	Clear	Lake-like	x	x	-
21	Xingu	Mud	Clear	Lake-like	x	-	-
22	Xingu	Mud	Clear	Lake-like	x	x	-
23	Pará	-	White	Estuarine channel	-	-	x
24	Pará	-	White	Estuarine channel	-	-	x
25	Pará	-	White	Estuarine channel	-	-	x
26	Amazon	Sand/Mud	White	Straight fluvial channel	-	x	-
27	Amazon	-	White	Straight fluvial channel	-	x	x
28	Amazon	-	White	Straight fluvial channel	-	-	x
29	Amazon	-	White	Straight fluvial channel	-	-	x
30	Amazon	Sand	White	Straight fluvial channel	x	-	-
31	Amazon	Sand	White	Straight fluvial channel	x	x	-
32	Amazon	Sand/Mud	White	Straight fluvial channel	-	x	-
33	Amazon	-	White	Estuarine channel	-	-	x
34	Amazon	-	White	Estuarine channel	-	-	x

[a] Location numbers refer to numbers of sampling locations in Figure 1.

[b] Seasons when site was measured.

Table 2. Number of sites per water season (h=high; l=low; f=falling), CH_4 concentrations in the water ($[CH_4]_{aq}$ µM)**,** diffusive fluxes, ebullition, total fluxes (mmol m^{-2} d^{-1}) and percentage of ebullition for rivers.

	Rivers								
	Negro	**Solimões**	**Preto**	**Madeira**	**Lake Curuai**	**Tapajós**	**Xingu**	**Amazon**	**Pará**
***n* Site/Season**	3l, 3h	3l, 3h	1h	3h	1f	4l, 3h, 1f	7l, 6h	2l, 4h, 5f	3f
$[CH4]_{aq}$									
Mean (± SD)	0.07±0.03	0.04±0.04	0.06	0.03±0.01	0.17	0.16±0.20	0.23±0.10	0.09±0.08	0.05±0.01
Median	0.08	0.03	0.06	0.03	0.17	0.05	0.24	0.08	0.06
Range	0.02-0.10	0.02-0.12	-	0.03-0.04	-	0.04-0.50	0.03-0.41	0.02-0.31	0.04-0.06
n	6	6	1	3	1	8	13	11	3
Diffusive flux									
Mean (± SD)	0.48±0.42	0.25±0.16	0.09±0.01	0.04±0.04	1.13±0.27	2.27±3.74	2.95±3.87	1.06±1.46	0.25±0.06
Median	0.32	0.26	0.09	0.02	1.07	0.55	1.35	0.37	0.25
Range	0.05-1.25	0.04-0.58	0.07-0.11	0.01-0.18	0.85-1.59	0.16-14.75	0.13-18.57	0.10-6.60	0.13-0.34
n	58	52	15	40	10	65	100	92	20
Total flux									
Mean (± SD)	0.54±0.56	0.31±0.35	0.09±0.01	0.04±0.04	1.13±0.27	2.41±4.10	5.96±9.15	1.35±2.15	0.31±0.31
Median	0.33	0.26	0.09	0.02	1.07	0.55	1.78	0.38	0.25
Range	0.05-3.36	0.04-2.54	0.07-0.11	0.01-0.18	0.85-1.59	0.16-16.14	0.13-40.26	0.10-10.03	0.13-1.62
n	58	52	15	40	10	65	100	92	20
Ebullition									
Mean (± SD)[1]	0.06±0.34	0.05±0.34	0	0	0	0.14±0.88	3.01±7.14	0.29±1.32	0.07±0.30
Range[2]	0.18-2.58	0.24-2.48	-	-	-	2.28-6.73	1.34-35.66	3.11-9.34	1.33
n chambers[3]	4	2	0	0	0	2	23	5	1
n occurence[4]	4	2	0	0	0	1	8	3	1
Ebullition (%)	11	17	0	0	0	6	51	22	21

[1] Total contribution of ebullition per river. The mean ebullition was calculated normalizing the area covered by all chambers used per site in the river, including those not receiving ebullition.
[2] Minimum and maximum ebullition captured in a single chamber per river
[3] Number of chambers receiving ebullition.
[4] Number of measurements where ebullition was found in at least one of the chambers.

Table 3. Total CH_4 flux versus sediment type, water type and season.

		Total flux (mmol m^{-2} d^{-1})					
		Mean	sd	Median	Min	Max	*n*
Sediment	Mud	4.9	8.3	0.9	0.07	40.3	133
	Mud/sand	1.2	2.2	0.3	0.05	10.0	80
	Non-identified	0.4	0.6	0.3	0.1	4.6	66
	Sand	0.9	2.2	0.3	0.01	19.2	173
Water type	Black	0.4	0.5	0.1	0.05	3.4	73
	Clear	4.6	7.7	0.9	0.1	40.3	165
	White	0.7	1.5	0.3	0.01	10.0	214
Season*	High water	0.9	1.3	0.3	0.04	13.0	161
	Low water	4.1	7.5	0.8	0.2	37.1	112

*Here we considered only sites sampled in both seasons (n = 16).
sd: standard deviation
n: number of measurements

Figure legends

Figure 1. Sites of flux measurements performed in different seasons and tributaries of the Amazon River system. The numbers in parentheses in the legend indicate how many sites were measured in each season. See Tables 1 and 2 for more site information.

Figure 2. Frequency distribution of the Calculated k_{600} / Minimum k_{600} ratio for the specific site and measurement period using floating chamber measurements, used for distinction between fluxes consisting of both ebullition and diffusion and those only of diffusiion. See text for details.

Figure 3. Diffusive fluxes (log transformed) between sites measured in each river. Numbers in the x axis are the sites showed in Figure 1 and Table 1. Letters above or below the boxes indicate the grouping of sites within each river based on a one-way ANOVA with Tukey's test ($p<0.05$) to determine which sites had similar emissions (e.g. Sites with an *a* in their letter combination were significantly different from those without an *a* in their combination).

Figure 4. Mean and standard deviation of diffusive flux and concentration of CH_4 in the cross-section profiles of the (a) Amazon and (b) Pará Rivers.

Figure 5. Log_{10} of total CH_4 flux (mmol m^{-2} d^{-1}) comparisons of sites in regards to (a) different types of sediments, (b) source river, (c) river water type, and (d) river water level (seasonal comparison performed with only sites measured during both seasons). Letters above graphics show grouping according to Tukey post-hoc test ($p<0.05$).

Figure 6. Seasonal total flux comparison per river considering only sites measured during both high (H) and low (L) water seasons.

Figure 7. Average CH_4 fluxes via diffusion and ebullition for each river. Error bars show the standard deviation.

Figure 8. (a) Ebullition according to depth and sediment type for each site it was observed; (b) Seasonal influence on ebullition. Individual chambers receiving ebullition was considered here.

Figure 1

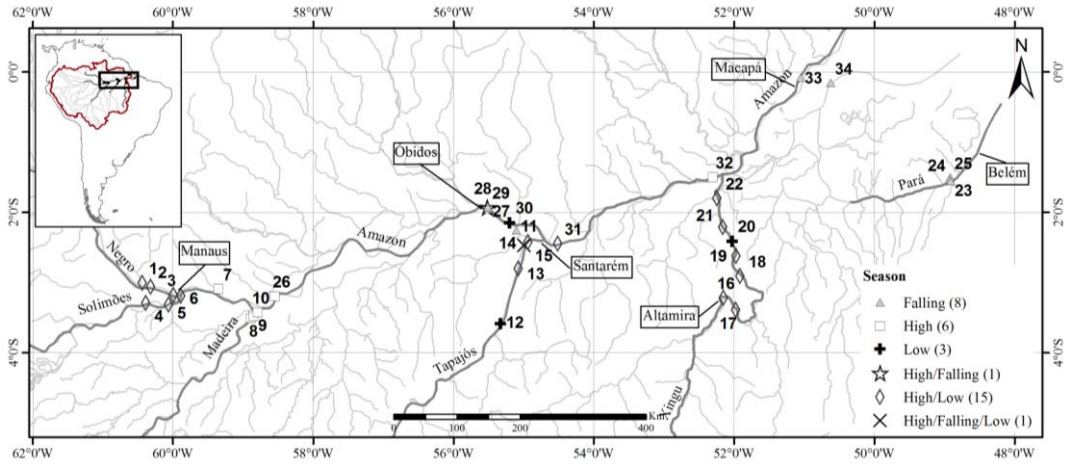
62°0'W
60°0'W
58°0'W
56°0'W
54°0'W
52°0'W
50°0'W
48°0'W
0°0'
2°0'S
4°0'S
N
Macapá
Amazon
Obidos
Amazon
Manaus
Negro
Solimões
Madeira
Santarém
Tapajós
Altamira
Xingu
Pará
Belém
Season
Falling (8)
High (6)
Low (3)
High/Falling (1)
High/Low (15)
High/Falling/Low (1)
0
100
200
400
Km

Figure 2

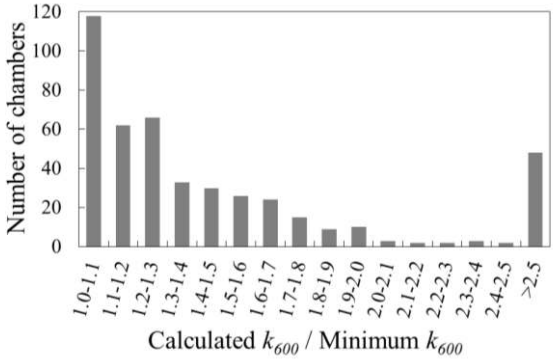
Number of chambers
120
100
80
60
40
20
0
1.0-1.1
1.1-1.2
1.2-1.3
1.3-1.4
1.4-1.5
1.5-1.6
1.6-1.7
1.7-1.8
1.8-1.9
1.9-2.0
2.0-2.1
2.1-2.2
2.2-2.3
2.3-2.4
2.4-2.5
≥2.5
Calculated k_{600} / Minimum k_{600}

Figure 3

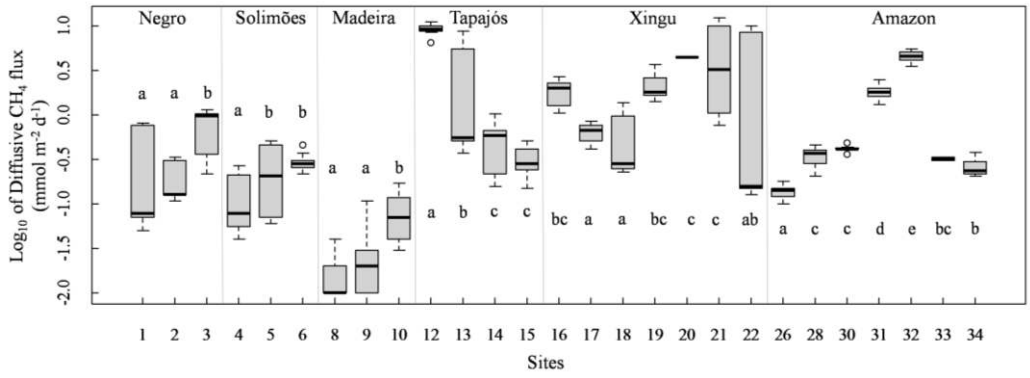
Negro
Solimões
Madeira
Tapajós
Xingu
Amazon
Log10 of Diffusive CH4 flux (mmol m-2 d-1)
1.0
0.5
0.0
-0.5
-1.0
-1.5
-2.0
a a b
a b b
a a b
a b c c
bc a a bc c c ab
a c c d e bc b
1 2 3 4 5 6 8 9 10 12 13 14 15 16 17 18 19 20 21 22 26 28 30 31 32 33 34
Sites

Figure 4

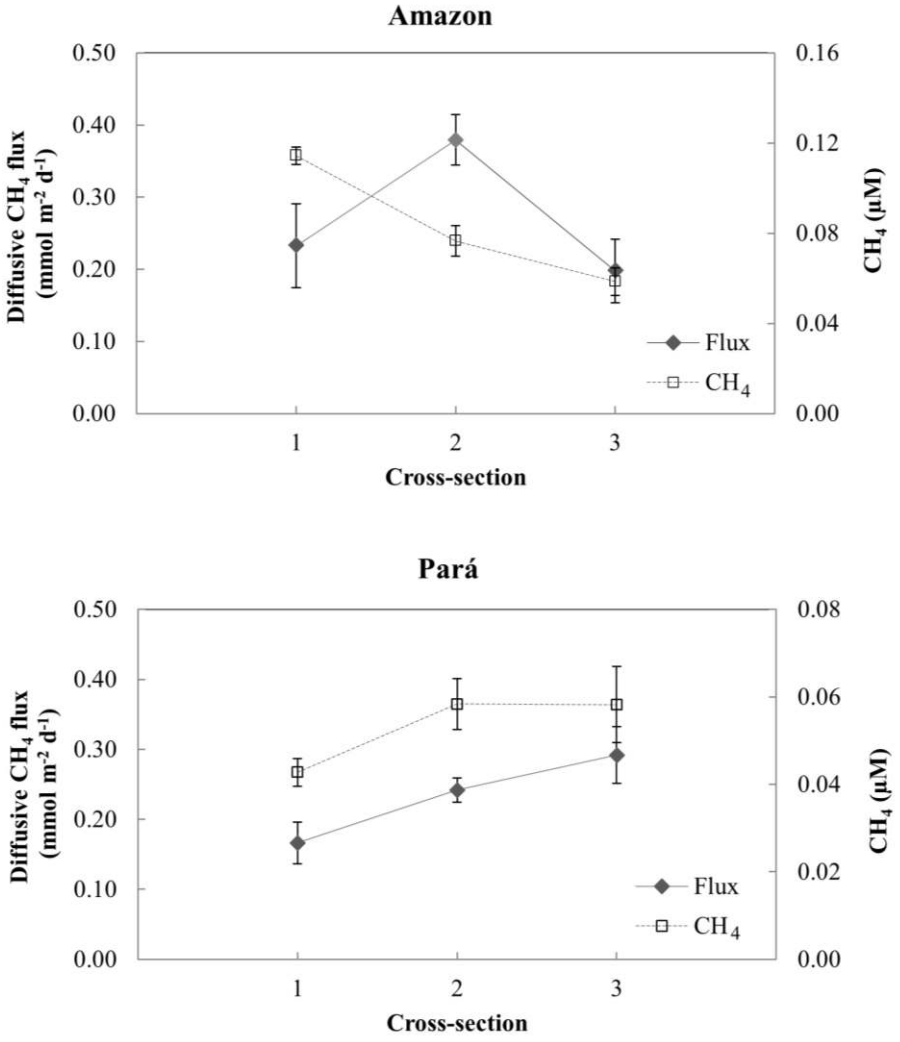
Amazon
Diffusive CH4 flux (mmol m-2 d-1)
CH4 (µM)
0.50
0.40
0.30
0.20
0.10
0.00
0.16
0.12
0.08
0.04
0.00
Flux
CH4
1
2
3
Cross-section
Pará
Diffusive CH4 flux (mmol m-2 d-1)
CH4 (µM)
0.50
0.40
0.30
0.20
0.10
0.00
0.08
0.06
0.04
0.02
0.00
Flux
CH4
1
2
3
Cross-section

Figure 5

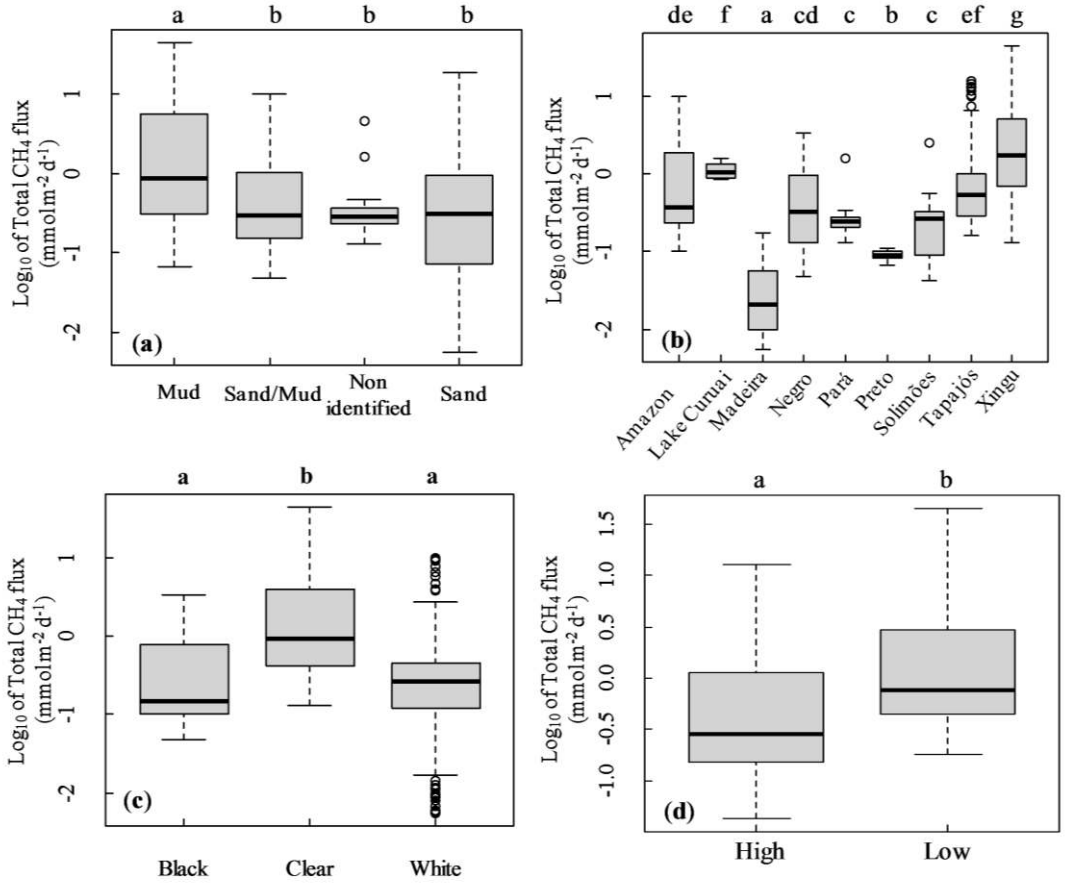
a
b
b
b
Log10 of Total CH4 flux (mmol m-2 d-1)
(a)
Mud
Sand/Mud
Non identified
Sand
de
f
a
cd
c
b
c
ef
g
(b)
Amazon
Lake Curuai
Madeira
Negro
Pará
Preto
Solimões
Tapajós
Xingu
a
b
a
(c)
Black
Clear
White
a
b
(d)
High
Low

Figure 6

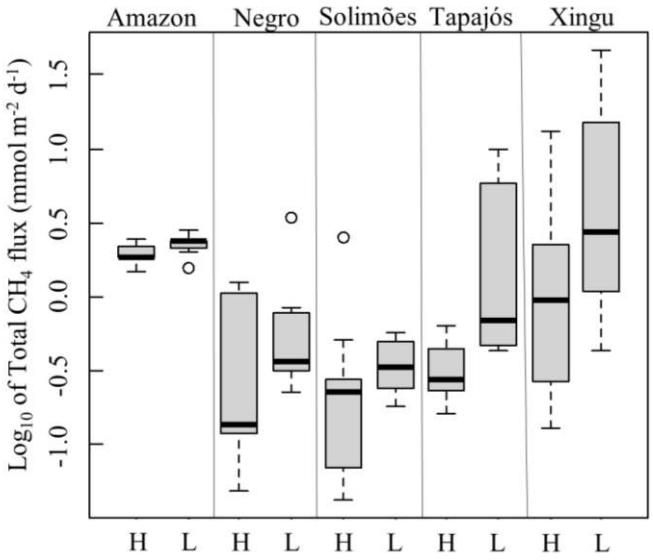
Amazon
Negro
Solimões
Tapajós
Xingu
Log10 of Total CH4 flux (mmol m-2 d-1)
-1.0
-0.5
0.0
0.5
1.0
1.5
H
L
H
L
H
L
H
L
H
L

Figure 7

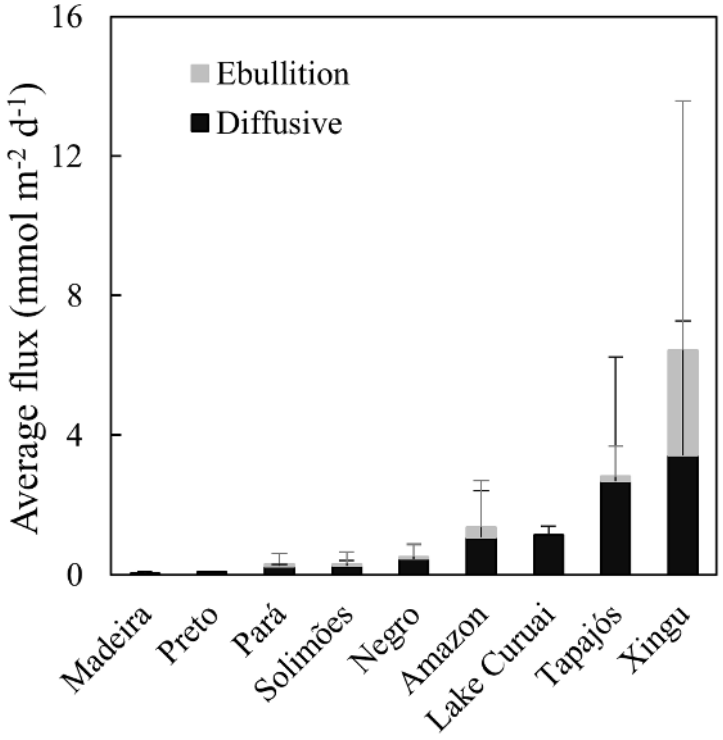
16
12
8
4
0
Average flux (mmol m-2 d-1)
Ebullition
Diffusive
Madeira
Preto
Pará
Solimões
Negro
Amazon
Lake Curuai
Tapajós
Xingu

Figure 8

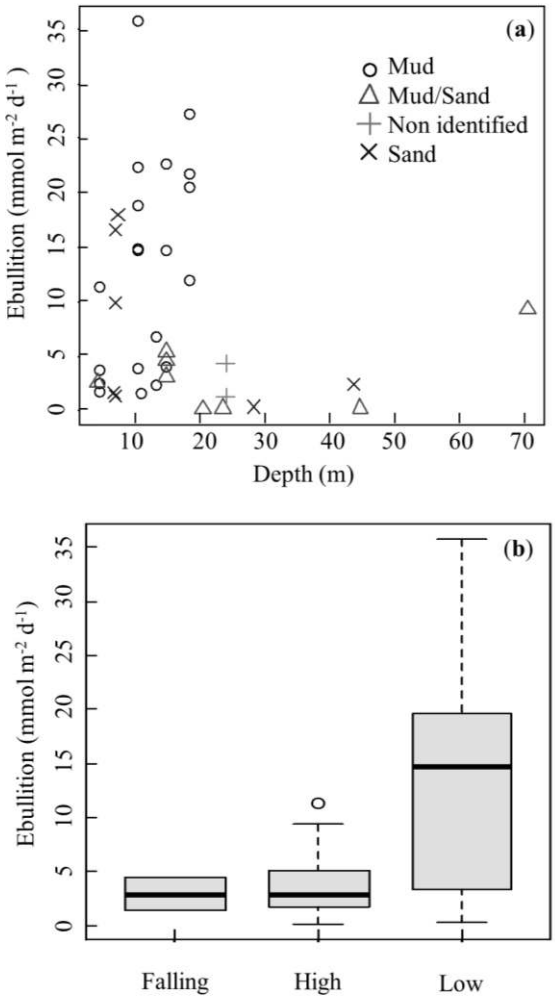
(a)
Mud
Mud/Sand
Non identified
Sand
Ebullition (mmol m-2 d-1)
Depth (m)
(b)
Ebullition (mmol m-2 d-1)
Falling
High
Low